Deleting Two-thirds of the C-terminus Alpha Domain Region in Autotransporter Antigen 43 is Associated with Increased Aggregation and Biofilm Formation in DH5α *Escherichia coli*

Lina Shalaby, Palak Tank, Ethan Wong, Dennis Xie

Department of Microbiology and Immunology, University of British Columbia, Vancouver, British Columbia, Canada

SUMMARY Antigen 43 is an autotransporter protein present in *Escherichia coli* associated with bacterial aggregation and biofilm formation. This protein is extensively studied due to its involvement in bacterial pathogenesis and antibiotic resistance. However, the specific role of the C-terminus alpha domain region of Antigen 43 in aggregation and biofilm formation has yet to be fully elucidated. In this study, we investigated the impact of deleting two-thirds of the C-terminus alpha domain region in Antigen 43 on aggregation and biofilm formation, specifically in the DH5α *Escherichia coli* strain. These DH5α cells were transformed with plasmids containing either full-length Antigen 43 (wild type) or the partially deleted Antigen 43 (mutant) construct and transformation was confirmed via western blot analysis. Aggregation assays were conducted using phosphate-buffered saline suspensions at pH 5, 6, and 7 for the wild-type strain and at a pH of 5 to compare between the wild type and mutant strains. Additionally, using a crystal violet assay, biofilm formation of the mutant strain was assessed and compared relative to the wild type strain. Our results demonstrated that Antigen 43 mutant cells exhibited greater aggregation compared to wild type and empty vector strains through observing cells clumping in test tubes and optical density readings in aggregation assays. Likewise, biofilm formation assays showed a similar trend, indicating enhanced biofilm formation in the mutant strain. These findings suggest that deletion of two-thirds of the C-terminus alpha domain region in Antigen 43 enhances aggregation and biofilm formation in DH5α *E. coli*. This prompts further investigation into the underlying mechanisms driving these observations and its implications for pathogenesis and antimicrobial resistance in bacterial cells displaying Antigen 43 on their cell surface.

INTRODUCTION

Type Va secretion systems, also known as classical autotransporters, are surface-localized proteins that cross the outer membrane (OM) autonomously; various virulence factors, such as adhesins in gram-negative bacteria are identified as autotransporters that increase pathogenesis (1). Antigen 43 (Ag43) is a notable autotransporter expressed by *agn43* (also called *flu*) found in bacterial strains within the Enterobacteriaceae family, including pathogenic *Escherichia coli,* such as uropathogenic *E. coli* (UPEC) (2, 3). Furthermore, Ag43 acts as a self-recognizing adhesin, facilitating the attachment of *E. coli* cells to various surfaces (4). Therefore, this autotransporter can enhance the ability of commensal and pathogenic *E. coli* to adhere to host tissues, neighboring bacterial cells, and other abiotic surfaces.

Ag43 has been shown to influence autoaggregation in liquid media (5). This is an important aspect of Ag43, as aggregation is a critical mechanism for bacterial resistance to host immune factors and antibiotics (6). Likewise, Ag43 is reported to promote biofilm formation, and thus improve resistance to antimicrobial agents (6). Because biofilms contribute to approximately 60–80% of microbial infections, they pose severe health complications in humans, and are considered the underlying cause for reducing the effectiveness of certain antimicrobial agents (7, 8). Similarly, Kjærgaard *et al.* observed the role of Ag43 in biofilm production using biofilm screening assays and flow chamber experiments. Their results revealed that Ag43 not only enhances biofilm production in *E. coli*, but also promotes interspecies biofilm formation between *E. coli* and *Pseudomonas*

Published Online: September 2024

Citation: Shalaby, Tank, Wong, Xie. 2024. Deleting two-thirds of the C-terminus alpha domain region in autotransporter Antigen 43 is associated with increased aggregation and biofilm formation in DH5α *Escherichia coli*. UJEMI 29:1-11

Editor: Shruti Sandilya and Ronja Kothe, University of British Columbia

Address correspondence to: https://jemi.microbiology.ubc.ca/

fluorescens (4). Ultimately, further studies to better understand Ag43 and similar autotransporters used in pathogenic *E. coli* strains is a key step to developing novel strategies for combating persistent and chronic bacterial infections.

Although the overall function of Ag43 has been studied, the role of the different structural regions within this autotransporter protein is not fully characterized. For this project, we aim to investigate the levels of autoaggregation and biofilm production of *E. coli* DH5α cells, upon deleting amino acids 193-551 of the C-terminal of the alpha domain in Ag43. This will allow the exploration of whether this specific region in the alpha domain is necessary for the aggregation and biofilm production function of DH5α bacterial cells, and will lead to further research moving forward on new strategies to potentially combat bacterial infections and control biofilm-related complications in various healthcare and industry settings.

As characterized previously by Owen *et al.*, Ag43 is composed of an N-terminal signal sequence, alpha domain (passenger domain), autotransporter, and C-terminal beta-barrel (9). The alpha domain of Ag43 (α43) folds into a right-handed three-stranded β-helix, forming an L-shaped protein with a twisted, irregular structure (9). This conformation, along with intricate networks of hydrogen bonds, contributes to the protein's aggregation function (8).

More recently, Najera Mazariegos *et al.* explored the effects of deleting two-thirds of the C-terminal Ag43 passenger domain (amino acids 193-551) in *E. coli* DH5α to observe changes in colony morphology and to better understand regional functional significance. However, Najera Mazariegos *et al.* concluded that the deletion of this region resulted in aggregation, contrary to previous literature (7,8,10).

Similar to Ag43, fimbriae are another surface protein present in *E. coli*. Due to fimbrae's long filamentous structure this protein also acts as appendages facilitating bacterial adhesion and colonization onto surfaces (11). However, these hair-like structures exert steric hindrance effects, physically obstructing the binding sites for other surface-associated proteins such as Ag43 (Figure 1) (12). Consequently, such steric hindrance can prevent Ag43 in mediating bacterial aggregation and biofilm formation (12). However, fimbriae expression is subject to phase variation, a reversible switch between distinct phenotypic states, where the *fimB* or *fimE* genes shift fimbriae expression from the "on" to "off" state (13). Therefore, different environmental conditions can lead to decreased fimbriae expression. Studies conducted by Schwan *et al.* highlighted the significance of environmental cues, such as low pH and high osmolarity, that can turn off fimbriae expression (14). Specifically, they found that under conditions of pH 5.5, and osmolarity of 400mM and 800 mM NaCl, the "*fim* off" phenotype is most prevalent (14). As a result, our study will also identify and consider optimal growth conditions that limit fimbriae expression to measure the aggregation and biofilm formation of DH5α strains affected by the Ag43 partial deletion.

Building on these insights, our study will investigate how aggregation and biofilm production is affected when Ag43 amino acids 193-551 of the C-terminal of the alpha domain are deleted. Furthermore, because Najera Mazariegos *et al.* (10) observed results that did not align with existing literature regarding Ag43 and its role in aggregation, our study also aims to perform confirmatory analyses while also taking into consideration methods to reduce fimbriae expression. Ultimately, we hypothesize that the deletion of amino acids 193-551 in the C-terminus alpha domain region in Ag43 will result in increased aggregation and biofilm production in the DH5α *E. coli* strain.

METHODS AND MATERIALS

Preparation of bacterial strains and growth conditions. The empty vector pBAD24 (EV), wild type transformed with plasmid pBAD-Ag43 (WT), and mutant transformed with plasmid pSMAK (MT) *E. coli* DH5α strains were cultured in Luria broth (LB) media at 37°C and 200 rpm of shaking overnight. Cultures were supplemented with 0.1 mg/mL of ampicillin to select for the EV, WT, and MT strains obtained from the MICB 471 lab, as provided by Najera Mazariegos *et al.* (10).

Plasmid extraction and transformation of *E. coli* DH5α cells. The pBAD24, pBAD-Ag43, and pSMAK plasmids were isolated from individual overnight cultures of *E. coli* DH5α EV, WT, and MT strains using the EZ-10 Spin Column Plasmid DNA Miniprep Kit (Bio Basic).

NanoDrop 2000 (ThermoFisher) was utilized to assess plasmid purity, and the extracted plasmids were stored at -20°C for downstream processing.

Commercially competent DH5α *E. coli* cells (Invitrogen) were transformed with pBAD24, pBAD-Ag43, and pSMAK plasmids through a heat-shock transformation protocol described by Chang *et al.* (15). Briefly, individual aforementioned plasmids were added to competent cells, followed by a 30-minute chilling period on ice. A quick heat shock treatment was performed at 42°C for 30 seconds and the cells were incubated on ice for two minutes. The transformed cells were then cultured in LB broth at 37°C with gentle shaking for one hour, after which they were plated onto LB agar plates containing ampicillin. Overnight incubation at 37°C allowed for the observation of transformed colonies the next morning.

Western blot. SDS-PAGE gels were prepared using the TGX Stain-Free FastCast Acrylamide Kit (10% Bio-Rad). 2x Laemmli sample buffer was created by mixing 2x Laemmli sample buffer (Bio-Rad) with beta-mercaptoethanol (BME) at a 10:1 ratio. Overnight cultures with EV, WT, and MT strains were then vortexed, centrifuged, and resuspended in 2x Laemmli sample buffer at a 1:1 ratio. Subsequently, the samples were heated to 95°C for five minutes before being loaded onto the SDS-PAGE gel.

Samples were stacked by running at 100V for 10 minutes, followed by resolution at 200V for one hour. Western transfer was conducted onto a PVDF membrane at 25V for one hour. Protein transfer confirmation was performed with Ponceau S staining, followed by washing with TBS-T and blocking for one hour at room temperature with TBS-T in 5% skim milk. TBS-T was utilized to wash the membrane between incubation steps.

The primary antibody, Anti-Ag43 (Flu), was diluted at 1:2000 in TBS-T and incubated overnight at 4°C (Cusabio). The secondary antibody, Goat Anti Rabbit IgG StarBright Blue 700, was diluted at 1:5000 in TBS-T and incubated covered for one hour at room temperature (Bio-Rad). After washing the membrane with TBS-T, imaging was performed using the StarBright B700 setting on the Bio-Rad ChemiDoc.

In place of preparing SDS-PAGE gels, Mini-PROTEAN TGX Stain-Free™ Precast Gels (Bio-Rad) were also used. Western transfer was conducted through the Bio-Rad Trans-Blot Turbo Transfer System onto Trans-Blot Turbo PVDF transfer packs, using the MIXED MW turbo setting at 25V for 7 minutes.

Aggregation assay with pH 5, 6, and 7 growth conditions in DH5α EV, WT, and MT strains. Overnight cultures of *E. coli* DH5α strains, including EV, WT, and MT, were grown in LB media at 37°C and 200 rpm in a shaking incubator. The subcultured strains were transferred into fresh LB media with a pH of 5, 6, and 7, adjusted by adding HCl prior to autoclaving, and incubated overnight again to reach an optical density reading at 600 nm (OD_{600}) of 0.9 to 1.0. Overnight cultures were induced with 1 mg/mL of L-arabinose two hours prior to the assay.

Prior to the aggregation assay, cell cultures were transferred to Oakridge tubes and ultracentrifugred for 10 minutes at 4000 rpm. The supernatant was discarded from the tubes and the pellet was resuspended by vortexing with an equivalent volume of PBS. The PBS also had an adjusted pH of 5, 6, and 7 depending on the experimental condition. 150 µL aliquots were transferred from the top of each culture tube into a 96-well plate for obtaining OD_{600} endpoint readings using the BioTek Epoch Microplate Spectrophotometer. Assays were conducted for durations between 50 to 90 minutes, with OD_{600} readings taken in 10-minute intervals. Variations included keeping cells on ice, measuring endpoint readings in shorter five-minute intervals, and testing pH conditions independently.

Crystal violet biofilm assay. The prepared DH5α EV, WT, and MT *E. coli* strains were used, grown in LB media with pH of 5 and 7, and the cultures were vigorously vortexed. Stationary phase cultures were diluted 1:100 into a fresh LB medium in triplicate to facilitate mean values for statistical analyses. 100 µL of diluted cultures were aliquoted into a sterile 96-well microtiter plate, including blank wells with uninoculated LB medium as a control. The plate was covered and incubated at 37°C for 24 hours. After 24 hours, OD_{600} reading was taken using the BioTek Epoch Microplate Spectrophotometer to measure cell density in each well.

For biofilm staining, planktonic cells were removed by inverting the plate over a waste tray and shaking gently. The plate was rinsed in clear water by rubbing its surface to release bubbles. Then, the plate was patted dry, and 125 µL of 0.1% crystal violet solution was added into each well and left for 10 minutes. The plate was inverted to remove excess liquid, rinsed, and patted dry. Biofilm formation was observed, and the plate was allowed to dry in the 37°C incubator for 15 minutes.

For quantification and measurement of biofilms, 150 µL of 30% acetic acid was added into each well to solubilize the biofilm. The plate was placed aside for 10 minutes, and well contents pipetted up and down for thorough stabilization. Subsequently, 125 µL of each sample was transferred to an optically clear, 96-well flat bottom plate (SARSTEDT, No. 82.1581.001). The biofilm expression was measured by conducting OD_{600} readings in a BioTek Epoch Microplate Spectrophotometer. OD_{600} readings from the crystal violet assay were normalized by dividing the OD_{600} readings from the crystal violet assay by the overnight cell density OD_{600} from each well.

RESULTS

Deleting the C-terminal two-thirds of the alpha domain of Ag43 leads to an increase in aggregation kinetics. N-terminal one-third of the alpha domain of Ag43 is critical in mediating the autoaggregation phenotype (16); however, as previously described by Najera Mazariegos *et al.* (10), *E. coli* with the C-terminal two-thirds deletion Ag43$\Delta_{(193\text{-}551)}$ have an increased aggregation kinetic. To replicate the differential aggregation kinetics observed by Najera Mazariegos *et al.*, we conducted a western blot analysis on the EV, WT, and MT cultures to confirm the presence of the deleted Ag43 in the mutant strain. Our findings revealed a prominent 70 kDa product in the WT lanes, with the signal intensity higher in the undiluted lanes compared with the 1/10 dilution lanes (Figure 1A). Additionally, a ~55 kDa

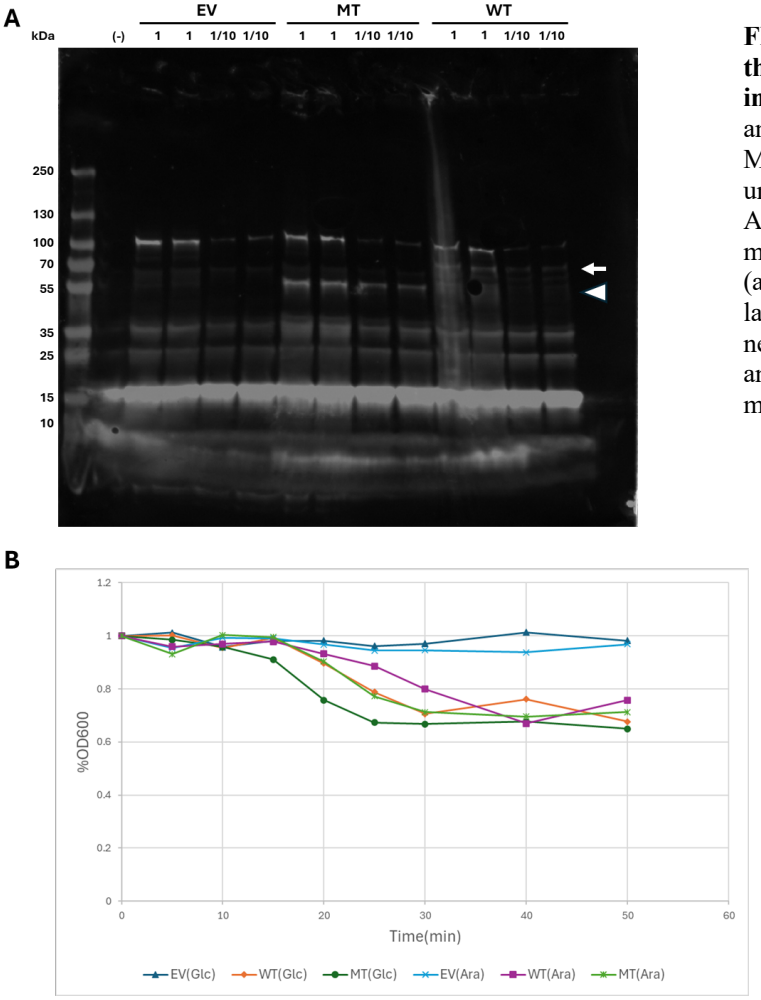

FIG. 1 Deletion of the C-terminal two-thirds of the alpha domain of Ag43 leads to an increase in aggregation kinetics. (A) Western blot using anti-Ag43 antibody and whole cell lysate of EV, MT, and WT. Each lane was loaded with either undiluted lysate or 1/10 diluted lysate. Wild type Ag43 was detected in WT lanes (arrow), while mutant Ag43 was detected in MT lanes (arrowhead), and no Ag43 was detected in EV lanes. Laemmli sample buffer was loaded as a negative control (-). (B) Aggregation of EV, WT, and MT strains of DH5α culture over time in liquid media.

product was detected in the MT lanes, with higher signal intensity in the undiluted lanes compared with the 1/10 dilution lanes (Figure 1A). Conversely, no bands corresponding to 70 kDa or 55 kDa were observed in the EV lanes, indicating that the bands detected in the WT and MT lanes likely represent Ag43 and Ag43 with a deleted region, respectively (Figure 2A). Subsequently, we determined the sedimentation rate of overnight cultures of EV, WT, and MT strains using OD_{600}. Our results indicated no aggregation in the EV strain under glucose and arabinose conditions (Figure 1B). Interestingly, WT and MT strains exhibited similar aggregation rates in both glucose and arabinose conditions, suggesting that the presence of glucose did not effectively inhibit Ag43 expression in this context. The MT strain displayed a higher aggregation rate in both conditions (Figure 1B). Overall, we confirmed the presence of mutant Ag43 in MT cells, and our aggregation assay results demonstrated an upward trend in aggregation kinetics in the MT strain. An important note is that the aggregation rate of DH5α *E. coli* cells demonstrated by Najera Mazariegos *et al.* (10) and here is low compared to other aggregation assays done on *E. coli* (3, 6, 8).

The influence of pH on Ag43-mediated aggregation. According to Hasman *et al.* (12), fimbriae expression is a physical steric that hinders autoaggregation mediated by Ag43. We hypothesize that the expression of fimbriae on DH5α cells might have hindered the aggregation observed (Figure 2). Previous studies showed that *E. coli* cells growing at a pH

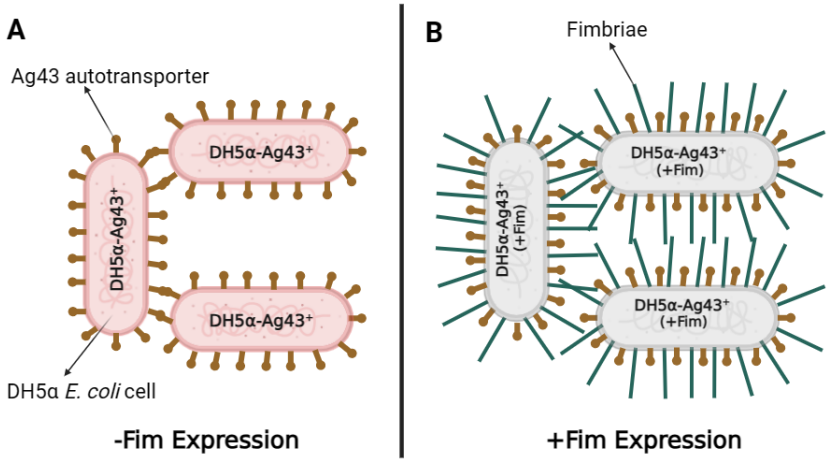

FIG. 2 A model displaying the relationship between fimbrial production and autoaggregation. (A) Ag43 mediates aggregation through self-interaction. (B) Expression of fimbriae on *E. coli* surface prevents interaction between Ag43 and thus preventing aggregation.

of 5 exhibited a fimbriae "off" phenotype (14). Here, we incubated *E. coli* cells in pH 5 PBS before the aggregation assay to reduce the effect of fimbriae on the aggregation kinetics. Our work revealed that WT cells incubated at pH 5 exhibited an increased aggregation rate compared with those incubated at pH 7 (Figure 3A). However, subsequent assays involving EV, WT, and MT strains did not consistently show the increasing effect of pH 5 on aggregation kinetics. The MT culture in the pH 7 condition exhibited an increased aggregation rate compared with the MT culture in pH 5 (Figure 3B). Additionally, WT and EV cultures in the pH 7 condition displayed similar aggregation kinetics to those in the pH 5 condition (Figure 3B). To further investigate the potential long-term effects of pH on aggregation, cultures of EV, WT, and MT were rested on the lab bench overnight at room temperature in either LB pH 7 or LB pH 5 conditions. Qualitative analysis of the overnight cultures revealed that EV, WT, and MT cultures in the pH 5 condition exhibited increased cellular aggregation at the bottom of the test tube when left undisturbed overnight (Supplementary Figure S1). MT cells also formed a larger pellet than WT cells in both conditions, further supporting our findings that MT cells have increased aggregation kinetic (Supplementary Figure S1). While our pH modulation trials yielded some insights, the overall consistency of using pH as a fimbriae modulator remains inconclusive. Interestingly, the effect of pH on fimbriae expression appears to impact long-term aggregation more significantly than short-term aggregation.

Higher biofilm production in mutant *E. coli* culture. The autoaggregation capacity of *E. coli* cells was closely associated with their ability to form biofilms (4). We employed a crystal violet assay to explore whether mutant *E. coli* strains exhibiting higher aggregation rates also demonstrate increased biofilm production. EV, WT, and MT cultures were grown

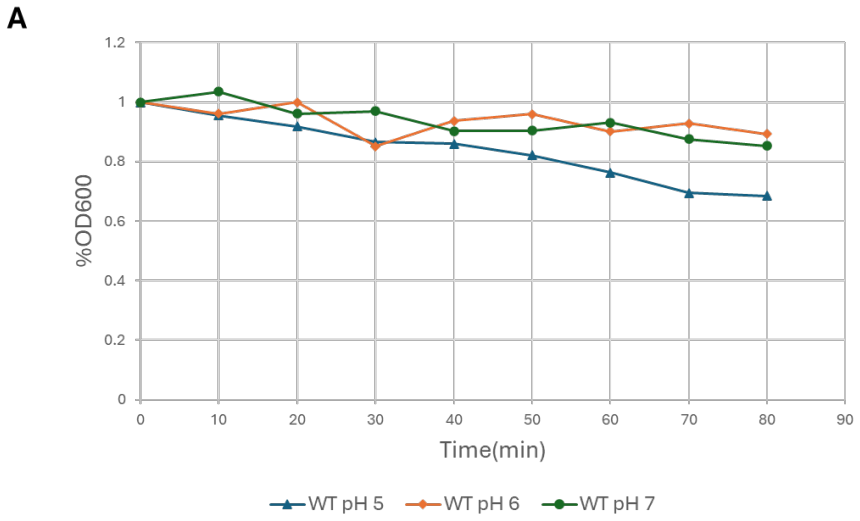

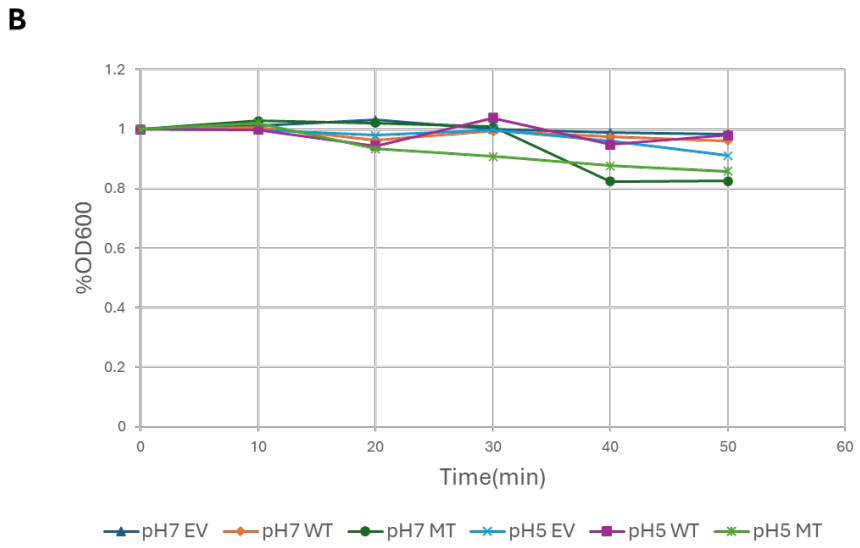

FIG. 3 The impact of pH on Ag43-mediated aggregation through fimbriae modulation. (A) Aggregation kinetics of WT strain in liquid culture at different pH conditions. (B) Aggregation kinetics of EV, WT, and MT in liquid culture at different pH conditions.

in a 96-well plate for 24 hours, after which the cells were removed, and crystal violet was added to stain the residual biofilm. Acetic acid was then applied to solubilize the crystal violet, and OD readings were evaluated to quantify biofilm production. We also incorporated pH 5 conditions, which allowed for the investigation of the effect of partial Ag43 alpha domain deletion on biofilm production in the absence of fimbriae expression. In LB conditions, we observed that WT strains exhibited nearly a three-fold increase in biofilm production compared to EV (Figure 4). Furthermore, biofilm production increased in the MT strain compared to the WT (Figure 4). Under pH 5 conditions, similar levels of biofilm production in WT and EV were observed (Figure 4). However, there was an increase in biofilm production in the MT strain compared to WT and EV (Figure 4). These results highlight the significance of Ag43-mediated autoaggregation in *E. coli* biofilm production, with the MT strain showing a higher aggregation rate correlating with increased biofilm production. Our findings also suggest that fimbriae expression in addition to Ag43 expression is required for biofilm production, as biofilm production dropped to levels similar to EV in pH 5 conditions. Moreover, the MT strain exhibited similar biofilm production in both LB and pH 5 conditions, suggesting that the mutation in the Ag43 alpha domain compensated for the loss of biofilm production in the absence of fimbriae.

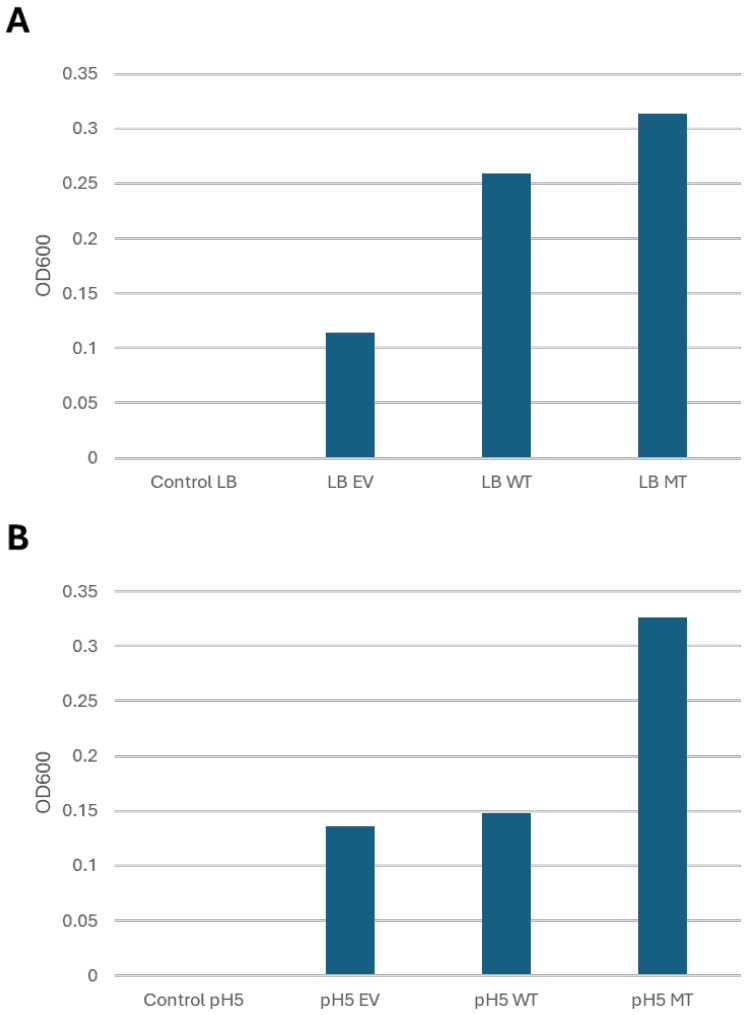

FIG. 4 Comparison of biofilm production in *E. coli* strains. (A) Biofilm production assessment by crystal violet staining for EV, WT, and MT strains grown in LB (pH 7) media overnight in a 96-well plate. (B) Biofilm production assessment by crystal violet staining for EV, WT, and MT strains grown in pH 5 media overnight in a 96-well plate. Crystal violet OD readings are normalized to the amount of cells in each well. Data represents results of one experiment.

DISCUSSION

To explore the effects of a partial deletion on the Ag43 passenger domain, we utilized the pSMAK plasmid construct created by Najera Mazariegos *et al.* (10). The western blot procedure using whole cell lysates of DH5α *E. coli* cells induced with 1 mg/mL arabinose were used to confirm the identity of the plasmids, and revealed strong bands at the 55 kDa position for our mutant cells and strong bands at 70 kDa for our wild type cells (Figure 1A). The relative positions of these bands were expected, with the mutant protein being lower in the gel than the wild type, although the exact size anticipated for the Ag43$\Delta_{(193\text{-}551)}$ mutant was larger than the reported 40 kDa (10). This discrepancy, along with the high position of the ladder end point in the gel and uneven horizontal distribution of lanes, suggested that the gel run time and handling techniques may have affected the accuracy of our results. Visible bands across all lanes at 100 kDa and the bright, white horizontal streaks below 35 kDa also suggest non-specific binding of the primary and secondary antibodies prior to imaging. Contamination is faintly visible in the negative control lane loaded with only Laemmli buffer. The large white streak visible in the leftmost WT lane was caused by a cell fragment being run through the gel, though this did not affect the migration of adjacent lanes in the gel. Based on these findings, we established the three cell types to be used in our subsequent assays.

Our initial confirmatory aggregation assay revealed similar trends in OD over time in both WT and MT cells, with the most rapid change decreasing between 15 and 25 minutes in both arabinose and glucose conditions (Figure 1B). The aggregation of cells measured indirectly through OD appeared to occur at similar rates for both of these cell genotypes, contradicting existing literature, and suggesting that a mutation in the alpha domain may prevent aggregation (8, 10). The assay was repeated on ice as well to eliminate the possibility of cells growing during the experiment and artificially increasing OD, but did not produce

notably distinct results. The minimal difference between arabinose and glucose induced cells also implies that the observed trends in OD may not be entirely dependent on the arabinose-induced plasmids containing the wildtype and partial deletion Ag43 genes. Hence, our initial results did not fully replicate the findings of Najera Mazariegos *et al.* (Figure 1B).

Consequently, the presence of fimbriae – with its known role in facilitating bacterial aggregation – was explored (11). The constitutive expression of fimbriae on the cell surface was suspected to play a role in sterically hindering WT and MT forms of Ag43 expressed on the cell surface as illustrated in Figure 2. To reduce fimbrial expression, an aggregation assay with pH 5 growth media was performed, and discovered that WT cells grown in pH 5 media demonstrated a lower final OD after 80 minutes compared with WT cells grown in pH 6 and 7 media (Figure 3A). These results aligned with the findings of Schwan *et al*., and suggested a downregulation of fimbriae or "*fim* off" phenotype was achievable through these environmental conditions (14). After repeating our assay with an experimental pH value of 5 and a control of unmodified LB at pH 7, we observed the greatest decrease in OD, and hence greatest aggregation in MT cells at a pH of 5 (Figure 3B). Between the initial 10 and 20 minute timepoints, a sharp decline in OD was observed in both pH 5 MT and pH 5 WT cells, although the endpoint OD of pH 5 MT was much lower at 50 minutes (Figure 3B). These results supported our hypothesis that the $Ag43\Delta_{(193\text{-}551)}$ cells would aggregate at a rate greater than WT. Growth of DH5α cells in pH 5 conditions appeared to be sufficient in inhibiting fimbriae interactions, and the need to do so in our experiment suggested that cell-to-cell aggregation was dependent on both Ag43-mediated and fimbriae-mediated interactions.

Interestingly, all LB-grown cells displayed similar trends in OD prior to the 30-minute timepoint, after which LB MT cells displayed the greatest change in OD within a 10-minute period amongst all experimental groups (Figure 3B). There was also inconsistency observed in the endpoints of pH 5 WT being higher than pH 5 EV, and that of pH 5 WT, LB EV, and LB WT being similar at the end of the 50-minute assay. The irregularity of these results could be a result of the limited time frame of the experiment and due to pipetting errors in the 96-well plates, which may have introduced variation in the OD readings from the spectrophotometer. Lastly, several of the initial aggregation assay trials were performed using frozen DH5α cells that had been thawed and subcultured on solid agar media, which were later replaced with a new batch of transformed DH5α cells. As such, our inability to replicate the findings of Najera Mazareigos *et al.* could be due to the viability of the experimental cells as opposed to our experimental procedure. Altering the salt concentration of our media to affect fimbriae expression was also conducted based on existing literature, though we did not observe noticeable changes in our results (14). Alternatively, the use of a *fim*-knockout strain may be more desirable, in case the mildly acidic environment pH was affecting the expression of Ag43 on the cell surface.

The crystal violet assay revealed the greatest biofilm production in MT cells compared with WT and EV cells, in both LB and pH 5 conditions (Figure 4A, 4B). These findings align with those from the aggregation assay, where MT cells had greater aggregation compared with LB, and suggest a relationship between aggregation rate and biofilm formation. Interestingly, the OD reading – and thus the mass of cells forming biofilms – for MT cells at pH 5 was approximately double that of WT and EV cells, while the latter two values were similar (Figure 4B). These results may suggest that the partial deletion of Ag43 may have a positive effect on the ability to form biofilms in acidic conditions. This may explain the 2-fold-decrease in OD for WT cells between LB and pH 5 conditions, suggesting WT Ag43 may have difficulty forming biofilms in acidic conditions. However, this does not account for why the OD for EV remained similar across both environmental conditions. The absence of OD readings in the control LB and pH 5 lanes acted as negative controls for the experiment, though the lack of repeated trials of this assay may have affected the reliability of the data. While convenient, the crystal violet staining method of choice is subject to experimental error, due to variability in the uptake of stain from bacterial cells and yield loss when resuspending the biofilm in acetic acid (17). Hence, other quantitative options such as fluorescent imaging techniques may provide more accurate readings for biofilm growth (18).

Limitations Although our results and analysis match the predictions made in our study hypothesis, it is important to note the several limitations within our study. One major

limitation to consider was the lack of access to knockout (KO) fimbriae *E. coli* cells. Despite our attempt to limit fimbriae expression by altering the growth conditions using pH, the presence of fimbriae was not entirely eliminated and thus fimbriae present in the cells could still potentially introduce steric hindrance effects on Ag43 and its binding abilities. As a result, this limitation could impact the interpretation of our results, as the observed effects of Ag43 on aggregation and biofilm may be influenced by the presence of fimbriae. Another limitation was the restricted duration of the aggregation assay, which was limited to a maximum of 90 minutes. This timeframe was based on the procedure by Klemm *et al.* (6) and selected as a feasible duration to conduct a continuous aggregation assay; however, this may not have captured the full extent of bacterial aggregation dynamics, potentially leading to an incomplete understanding of the role Ag43 may have in this process. Additionally, the inability to achieve an optimal OD of 1.0 prior to the aggregation assay may suggest suboptimal bacterial growth conditions and does not match or fully confirm the findings from Najera Majeriozos *et al*. (10). This limitation may affect the reproducibility and accuracy of our results, as bacterial growth deficiencies could impact Ag43 expression and subsequent aggregation behavior. Overall, addressing and controlling for these limitations in future research will ameliorate our understanding of Ag43-mediated aggregation and biofilm production in *E. coli* DH5α cells and beyond.

Conclusions Using the plasmid construct, pSMAK, containing the C-terminal two-thirds deletion of the Ag43 alpha domain, transformed DH5α cells displayed greater qualitative aggregation rates and biofilm formation compared to cells transformed with wild-type pBAD-Ag43. Aggregation assays demonstrated the greatest aggregation rate in MT strains, particularly in acidic conditions of pH 5. However, in pH 7 conditions, there was more consistency between the aggregation levels of the WT and MT strain. We hypothesized that the similar aggregation levels in pH 7 growth conditions were due to the steric hindrance from fimbriae which are constitutively expressed by DH5α *E. coli* cells and physically block Ag43 binding. Therefore, by altering the pH conditions to 5, fimbriae expression was reduced. Furthermore, through the crystal violet assay, MT cells exhibited higher biofilm production relative to the WT strain. Nonetheless, further confirmatory tests and independent studies are necessary to confirm the differences between Ag43$\Delta_{(193\text{-}551)}$ cells and WT cells on both aggregation and biofilm production.

Future Directions Based on the findings and limitations of this study, there are still several avenues to explore in order to enhance our understanding of Ag43 and its impact on aggregation and biofilm production. For example, conducting repeat experiments of the aggregation assay and crystal violet tests using fimbriae knockout *E. coli* cells would provide valuable insights into the specific role of Ag43 in bacterial aggregation, and eliminate potential steric hindrance effects from fimbriae. Moreover, obtaining double knockout cells of fimbriae and Ag43, then retransforming with the respective plasmids used in this study may validate the observed effects and ensure the observed aggregation and biofilm results are precisely due to the full-length or partially deleted Ag43 inserted within the cells.

Furthermore, continuing to explore different media conditions, including variations in pH and osmolarity, would support the confirmation of whether these environmental factors influence Ag43-mediated aggregation and biofilm formation. Although our study focused on pH variations, future studies may investigate ideal temperatures and osmolarity levels that support Ag43 expression in *E. coli* cells. Additionally, due to time limitations, our study was unable to explore aggregation kinetics adapted from the study by Klemm *et al*. (6) Future studies can design various Ag43 kinetics aggregation tests with, for example, 1:1, 1:2, 1:3, and 1:4 mix of mutant and WT cells to analyze the impact a mutant strain may have on aggregation within a group of cells. Consequently, performing Ag43 kinetics aggregation tests can highlight the interaction between WT and MT cells with distinct Ag43 and reveal the implications of adding mutant strains on aggregation within a growing bacterial population.

Moreover, future studies may also assess the pathogenicity of the mutant strain relative to the WT strain in vivo using mouse models or other mammalian cells. This would provide valuable insights regarding how this partial deletion of Ag43 may influence bacterial

virulence and disease progression. Additionally, investigating other distinct regions of Ag43 for deletion could uncover novel insights into additional domains important for Ag43-mediated aggregation and biofilm formation. These future directions can help further elucidate the complex interplay between Ag43, bacterial aggregation, and pathogenicity, and ultimately lead to new development of targeted therapeutic strategies against biofilm-associated infections of bacteria displaying Ag43.

ACKNOWLEDGEMENTS

We would like to thank Dr. David Oliver, Brynn McMillan, Jade Muileboom, and the entire MICB 471 teaching team for their valuable mentorship and support throughout this project. Additionally, we extend our thanks to the UBC Department of Microbiology and Immunology for their generous funding and provision of resources essential to reach our project milestones. We also express our appreciation and gratitude to our fellow classmates for their collaborative efforts and support during this project.

CONTRIBUTIONS

LS: Abstract, Introduction, Study Limitations, and Future Directions. Edited overall manuscript.
PT: Methods and Figures. Edited overall manuscript.
EW: Discussion and Conclusion. Edited overall manuscript.
DX: Results and Figures. Edited overall manuscript.

REFERENCES

1. **Leo JC, Grin I, Linke D.** 2012. Type V secretion: mechanism(s) of autotransport through the bacterial outer membrane. Philosophical Transactions of the Royal Society B 367:1088–1101. doi:10.1098/rstb.2011.0208
2. **Wallecha A, Oreh H, Van Der Woude MW, deHaseth PL.** 2014. Control of Gene Expression at a Bacterial Leader RNA, the *agn43* Gene Encoding Outer Membrane Protein Ag43 of *Escherichia coli*. Journal of Bacteriology 196:2728–2735. doi:10.1128/jb.01680-14
3. **Ulett GC, Valle J, Beloin C, Sherlock O, Ghigo J, Schembri MA.** 2007. Functional Analysis of Antigen 43 in Uropathogenic *Escherichia coli* Reveals a Role in Long-Term Persistence in the Urinary Tract. Infection and Immunity 75:3233–3244. doi:10.1128/iai.01952-06
4. **Kjærgaard K, Schembri MA, Ramos C, Molin S, Klemm P.** 2000. Antigen 43 facilitates formation of multispecies biofilms. Environmental Microbiology 2:695–702. doi:10.1046/j.1462-2920.2000.00152.x
5. **Henderson IR, Meehan, Owen.** 1997. Antigen 43, a phase-variable bipartite outer membrane protein, determines colony morphology and autoaggregation in *Escherichia coli* K-12. FEMS Microbiology Letters 149:115–120. doi:10.1111/j.1574-6968.1997.tb10317.x
6. **Klemm P, Hjerrild L, Gjermansen M, Schembri MA.** 2004. Structure-function analysis of the self-recognizing Antigen 43 autotransporter protein from *Escherichia coli*. Molecular Microbiology 51:283–296. doi:10.1046/j.1365-2958.2003.03833.x
7. **Coenye T, Nelis H.** 2010. In vitro and in vivo model systems to study microbial biofilm formation. Journal of Microbiological Methods 83:89–105. doi:10.1016/j.mimet.2010.08.018
8. **Heras B, Totsika M, Peters KM, Paxman JJ, Gee CL, Jarrott R, Perugini MA, Whitten AE, Schembri MA.** 2013. The antigen 43 structure reveals a molecular Velcro-like mechanism of autotransporter-mediated bacterial clumping. Proceedings of the National Academy of Sciences of the United States of America 111:457–462. doi:10.1073/pnas.1311592111
9. **Owen P, Caffrey P, Josefsson L.** 1987. Identification and partial characterization of a novel bipartite protein antigen associated with the outer membrane of *Escherichia coli*. Journal of Bacteriology 169:3770–3777. doi:10.1128/jb.169.8.3770-3777.1987
10. **Najera Mazariegos A, McDonald K, Tepes M, Zhang S.** 2023. Morphological and functional characterization of the C-terminal two-thirds of the autotransporter Ag43 alpha domain via site-directed mutagenesis in *Escherichia coli* DH5α. UJEMI.
11. **Klemm P.** 2004. Fimbriae: adhesion, genetics, biogenesis, and vaccines. Nat Rev Microbiol 2(5):363-378.
12. **Hasman H, Chakraborty T, Klemm P.** 1999. Antigen-43-mediated autoaggregation of *Escherichia coli* is blocked by fimbriation. *Journal of bacteriology*, *181*(16), 4834–4841. doi.org/10.1128/JB.181.16.4834-4841.1999.
13. **Kuwahara H, Myers CJ, Samoilov MS.** 2010. Temperature control of fimbriation circuit switch in uropathogenic *Escherichia coli*: quantitative analysis via automated model abstraction. *PLoS computational biology*, *6*(3), e1000723. doi.org/10.1371/journal.pcbi.1000723.

14. **Schwan WR, Lee JL, Lenard FA, Matthews BT, Beck MT.** 2002. Osmolarity and pH growth conditions regulate *fim* gene transcription and type 1 pilus expression in uropathogenic *Escherichia coli. Infection and immunity*, *70*(3), 1391–1402. doi.org/10.1128/IAI.70.3.1391-1402.2002.
15. **Chang AY, Chau VY, Landas JA, Pang Y.** 2017. Preparation of calcium competent *Escherichia coli* and heat-shock transformation. *JEMI Methods* Vol. 1:22-25.
16. **Van Der Woude MW, Henderson IR.** 2008. Regulation and Function of Ag43 (Flu). *Annu Rev Microbiol* 62:153–169.
17. **Shukla SK, Rao TS.** 2017. An improved crystal violet assay for biofilm quantification in 96-well microtitre plate.
18. **Jun W, Kim MS, Lee K, Millner P, Chao K.** 2009. Assessment of bacterial biofilm on Stainless Steel by hyperspectral fluorescence imaging. Sensing and Instrumentation for Food Quality and Safety 3:41–48.